1*H*-azepine-2-oxo-5-amino-5-carboxylic Acid: a 3_{10} Helix Inducer and a New Tool for Functionalized Gold-Nanoparticles

Sara Pellegrino †, Andrea Bonetti †, Francesca Clerici †, Alessandro Contini †, Alessandro Moretto§, Raffaella Soave ‡, and Maria Luisa Gelmi †*

KEYWORDS: alpha,alpha disubstituted amino acids, functionalized gold nanoparticles, 3_{10} helix, peptidomimetics

ABSTRACT

The asymmetric synthesis of 1*H*-azepine-2-oxo-5-amino-5-carboxylic acid, (**oxo-Azn**), a new α,α-disubstituted cyclic glutamine analogue was performed using an efficient "one-pot" asymmetric Schmidt reaction, between 4-disubstituted-cyclohexanone and 1,2-hydroxyethylazides, in the presence of a Lewis acid. The main (R) isomer was inserted at the *N*-terminus in a very short peptide sequence, *i.e.* PhCO-(R)-Oxo-Azn-L-Ala-Aib-L-AlaNHMe. A stable 3_{10}-helix conformation was obtained, as verified by both NMR experiments and molecular dynamics (MD) simulations. Finally, covered chiral gold nanoparticles have been prepared and fully characterized.

Introduction

Small molecules functionalized gold nanoparticles (GNPs) are at the forefront of the research in nano chemistry.[1] The three dimensional self-assembled monolayers constructed by the introduction of organic compounds on GNPs have emerged as versatile tools of surface modification. Furthermore, the organic monolayer reduces the surface energy of GNPs and thus provides increased solubility and colloidal stability.[2]

Amino acids and peptides are effective building blocks to create hierarchical nanomaterials [3] and functionalized GNPs[4]. They feature a multitude of functionalities and unique secondary structures based on controllable primary sequences and environmental conditions.[5] By using amino acids and peptides, it is thus possible to tailor new hybrid materials for a broad range of applications in different areas, such as medicine, bionanotechnology, and electrochemistry.[6]. On the other hand, focusing on biomedical applications, the peptide instability toward proteases might be a concern. Synthetic analogs of natural amino acids represent valuable tools to overcome this problem.[3b,7] In particular, the use of α,α-disubstituted derivatives gives the double advantage of reducing the metabolic degradation, and of stabilizing the helical conformation, by reducing the available conformational space of the peptide backbone.[8]

Continuing our researches on unnatural constrained amino acids[9], we, recently, prepared a α,α-disubstituted ornithine analogue, *i.e.* 1*H*-azepine-4-amino-4-carboxylic acid **Azn**, as an effective 3_{10}-helix inducer.[9c] Here we report on the asymmetric synthesis of 1*H*-azepine-2-oxo-5-amino-5-carboxylic acid, named **oxo-Azn**, a α,α-disubstituted cyclic glutamine analogue, containing on the nitrogen side chain a hydroxy tethering group (Figure 1). This functionalization is of particular relevance as it gave the possibility to exploit the use of the new scaffold for the preparation of gold nanoparticles.

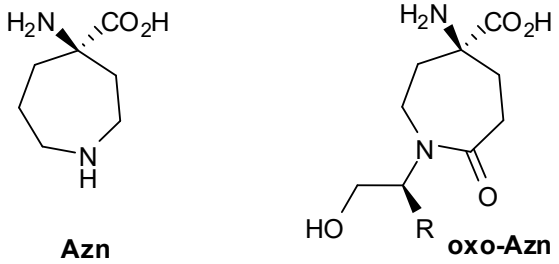

Figure 1. Azn and **Oxo-Azn**

Oxo-Azn was prepared using a very efficient one-step synthetic protocol that gives a mixture of "quasi enantiomers", easily separated by chromatography (Scheme 1). The main (R) isomer was thus inserted at the *N*-terminus in a very short peptide sequence, *i.e.* PhCO-(R)-Oxo-Azn-L-Ala-Aib-L-AlaNHMe. A stable 3_{10}-helix conformation was obtained, as verified by both NMR experiments and molecular dynamics (MD) simulations. Finally, taking advantage of the tethering group, covered chiral gold nanoparticles have been prepared and fully characterized.

RESULTS AND DISCUSSION

Synthesis of Oxo-Azn scaffold. 1*H*-azepine-2-oxo-5-amino-5-carboxylic derivatives **5/6** were synthesized through an asymmetric Schmidt reaction[10] on cyclohexanone **1**[9c] and 2 substituted 1,2-hydroxyethylazides (**2a,b**) (Scheme 1) The reaction was performed in CH_2Cl_2 and in the presence of an excess of $BF_3{\cdot}OEt_2$ (from -80 to 25 °C). After 48 h, the reaction was quenched with 2N NaOH affording a mixture of "quasi enantiomers" **5** and **6** (**a**: 67:33, 80%; **b**: 50:50, 75%; ^{1}H NMR and HPLC analyses). (Scheme 1). A similar diastereoselection and yield were obtained by changing the temperature (from -10 to 25 °C) and the reaction time (18 h).

To gain insight on the mechanism and diastereoselection, the reaction between **1** and **2a** was monitored by ^{1}H NMR. After 18 h, ^{1} H NMR analysis of the crude before NaOH quenching, showed the formation of intermediates **3a**/**4a** in 67:33 ratio. This mixture was crystallized from Et_2O affording the pure bicyclic intermediate **4a** (13%, for NMR discussion and crystallographic data see Supporting Information). Pure azepinone derivatives **5a** (45%) and **6a** (10%) were isolated after column chromatography of the mother liquors. (Scheme 2). Finally, the treatment of **4a** with NaOH (2N, 24 °C, 30 min.) gave the minor stereoisomer **6a** in quantitative yield. (Scheme 1)

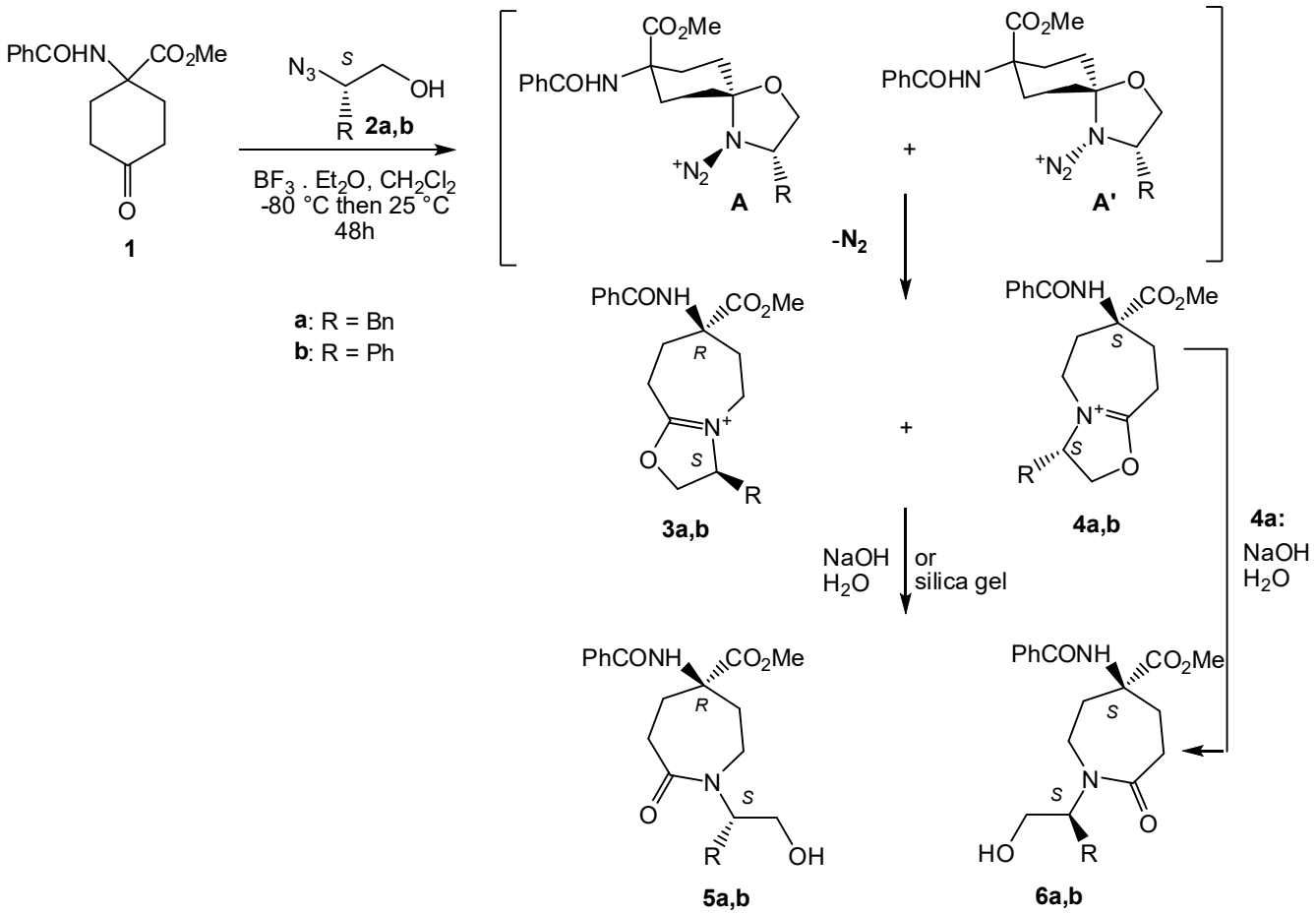

Scheme 1. Asymmetric Schmidt reaction on ketone **1**.

The isolation of the rigid bicyclic intermediate **4a** allowed to confirm that the mechanism of formation of "quasi enantiomers" **5/6** is the one proposed by Aubè et al. [10] Accordingly, the azidoaddition on ketone **1** affords a couple of diastereoisomeric spiro intermediates **A** and **A'** that differ for the stereochemistry of nitrogen leaving group. Consequently to the departing of N_2, the antiperiplanar migration of the methylene group of cyclohexyl ring occurs affording, from **A**, bicyclic salt **3**, and from **A'**, salt **4**. (Scheme 1)

Although the reaction occurred via the same mechanism, we found a different distribution of the diastereomers, with respect to literature data on 4-mono-substituted cyclohexanone. As reported by Aubè et al [10a] the Schmidt reaction between 4-*tert*-butylcyclohexanone and azide **2b** leads to a S diastereoselection through the

stabilization of intermediate **A'** by cation-π interaction. In our case no diastereoselection was observed, suggesting that steric factors drive the diastereoselction outcome. This hypothesis is confirmed by the partial diastereoselction found in the case of azide **2a**, containing the more flexible benzyl substituent. In this case, the minimization of steric interactions between the migrating methylene group and the benzyl substituent favours the formation of intermediate **3a** with respect to **4a**.

Synthesis of tetrapeptide PhCO-(R)-Oxo-Azn-L-Ala-Aib-L-AlaNHMe. First, the reaction between ketone **1** and azide **2a** was scaled up to 11g of starting material, yielding **5a** and **6a** in 85% yield (67:33 ratio). Column chromatography of the crude reaction mixture afforded the first diastereoisomer **5a** in 47% yield and the minor one **6a** in 23% yield.

The model peptide PhCO-(R)-Oxo-Azn-L-Ala-Aib-L-AlaNHMe was then prepared starting from α,α-amino acid **5a** (Scheme 2). *R*-isomer was selected since it is known that only the R-**Azn** isomer, (see Figure 1), is able to induce a 3_{10}-helix when inserted in a short pentapeptide containing L-amino acids.[9c]

First, the ester function on scaffold **5a** was hydrolyzed using a methanolic solution of NaOH (2N) in CH_2Cl_2/MeOH (9:1, 25 °C, 15h). Acid **7** was isolated in 95% yield. Compound **7** was made to react with alanine benzyl ester *p*-toluenesulfonate [HOAt (1equiv.)/EDC (1equiv.)/DIPEA (2 equiv.), CH_2Cl_2 25 °C, 2 h] affording dipeptide **8** (58% yield). The yield of **8** were increased (80%) using the free amine derivative of alanine operating with the same condensative conditions (15h). The benzyl group of the ester function was removed by hydrogenolysis (Pd/C, MeOH, 25 °C, 24h) giving acid **9** (90%, Scheme 3). The final tetrapeptide **10** (50%) was obtained by reaction of **9** with dipeptide H_2N-Aib-*L*-Ala-CONHMe [HOAt (1equiv.)/EDC (1equiv.)/DIPEA(2 equiv.), CH_2Cl_2 25 °C, 15 h]. Any attempt to synthesized directly compound **10** from **5a** and H_2N-*L*-Ala-Aib-*L*-Ala-CONHMe tripeptide failed, probably for the steric hindrance on the carboxylic function of **7**.

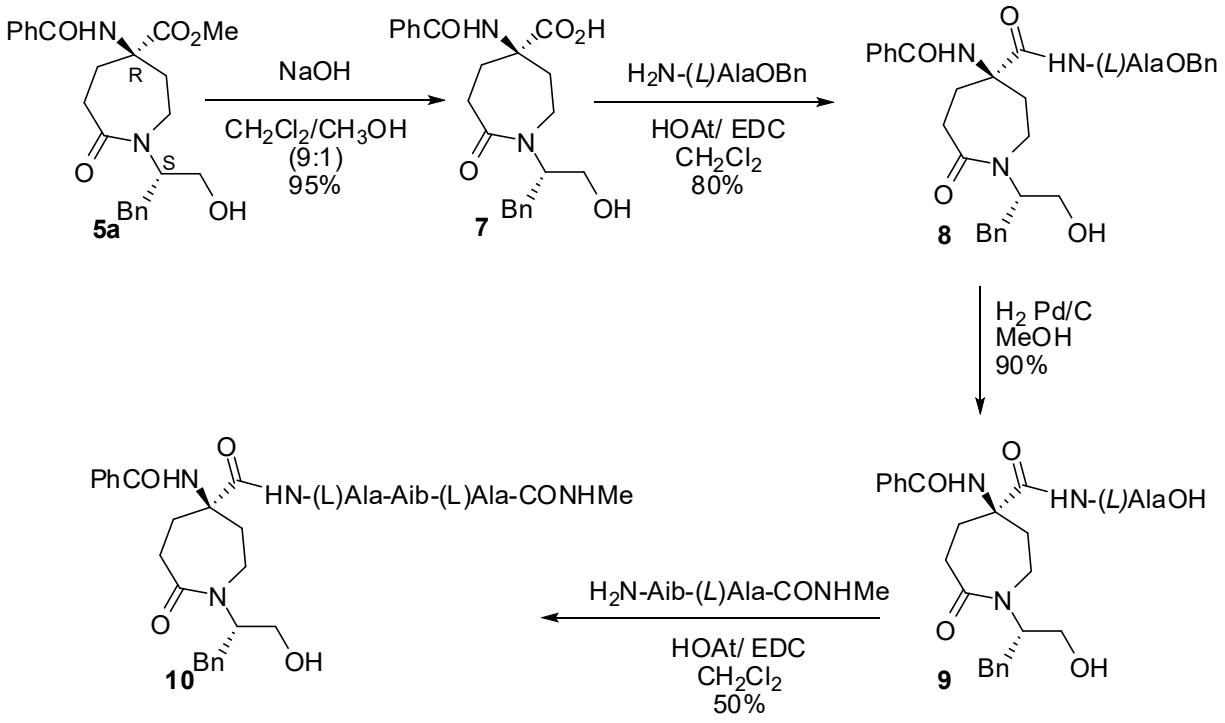

Scheme 2. Synthesis of tetrapeptide PhCO-(R)-Oxo-Azn-L-Ala-Aib-L-AlaNHMe

Tetrapeptide **10** was first purified by preparative RP-HPLC. During the purification we observed the formation of a by-product, corresponding to the bicyclic derivative **11** (Figure 3; see supporting information for NMR discussion). Its formation must be ascribed to the TFA present in the HPLC eluent phase that catalysed the dehydration/oxazoline ring formation. To overcome this issue, compound **10** was purified by crystallization of the crude reaction mixture.

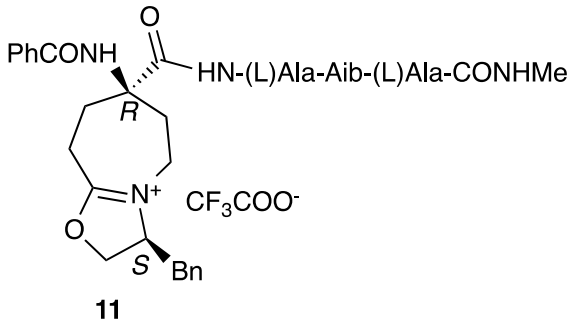

Figure 3. Product of transformation of **10** in acidic conditions

*NMR conformational studies on model peptide **10**.* A full assignment of the protons of peptide **10** was accomplished by 500 MHz NMR analysis (1H, ^{13}C, COSY, TOXY and HSQC NMR experiments, see Supporting Information). 2D-NOESY at different mixing times and temperature-dependent chemical shift variations experiments (from 273 to 333 K) were performed in CD_3CN solution, to obtain detailed information on the conformational behavior of **10**.

A complete set of N,N (i,i + 1) NOE cross-peaks [PhCONH/Ala-2 (w); Ala-2/Aib (m); Aib/Ala-4(vs)] were detected excepting for Ala-4/MeNH that are overlapped (Figure 5A).

A) B)

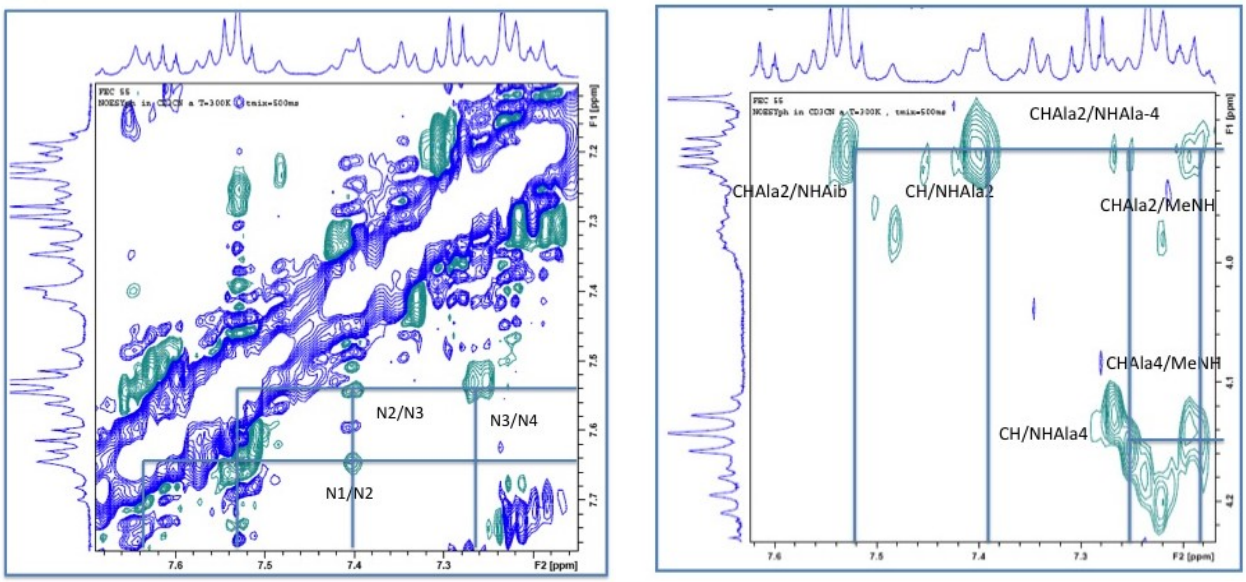

Figure 5. A) NH/NH and B) α,N N.o.e. regions (500 ms) for peptide **10**

Various NOEs are operative in the peptide chain, i. e. α,N (i,i+1) between Ala-2/Aib (m), and Ala-4/NHMe (w). (Figure 5B) Longer range α,N (i,i+2) and α,N (i,i+4)NOEs allow to define the helix types: the former is typical of a 3_{10}-helix, while the latter is typical of an α-helix[9c]. In our case, of relevance, are the long range N.o.e of Ala-2/Ala-4 [α,N(i,i+2; w), (Figure 5B) and of the aryl ring of benzyl moiety (δ 7.94) and the methyl of Aib (δ 1.54, m) (Figure 6). A further long range Noesy was detected between Ala-2 and NHMe [α,N(i,i+3; m)]. All these data are in agreement with a 3_{10}-helix conformation.

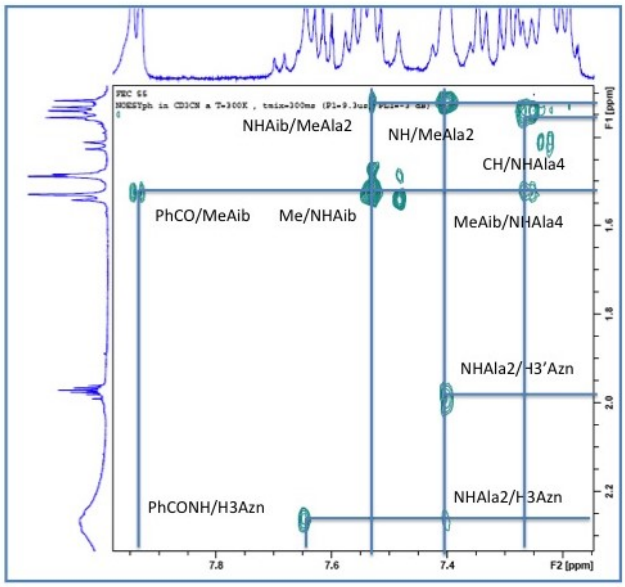

Figure 6. NH/β-H N.o.e. region (300 ms) for peptide **12**

^{13}C values of the anysotropic Me of Aib that are in a magnetically inequivalent environment such as in a helix structure, differ of more than 2 ppm[11]. In our case δ ^{13}C values of 23.0 and 26.3 were found for Aib-Me groups. NH chemical shifts temperature dependences, providing information on inaccessible or intramolecular H-bonds[9c] confirmed the helix structure, too. Values of -3.98 ppb K^{-1} for Oxo-Azn, -3.99 ppb K^{-1} for Ala-2, -2.57 ppb K^{-1} for Aib, -1.55 ppb K^{-1} for Ala-4 and -2.64 ppb K^{-1} for NHMe were detected (Figure 7).

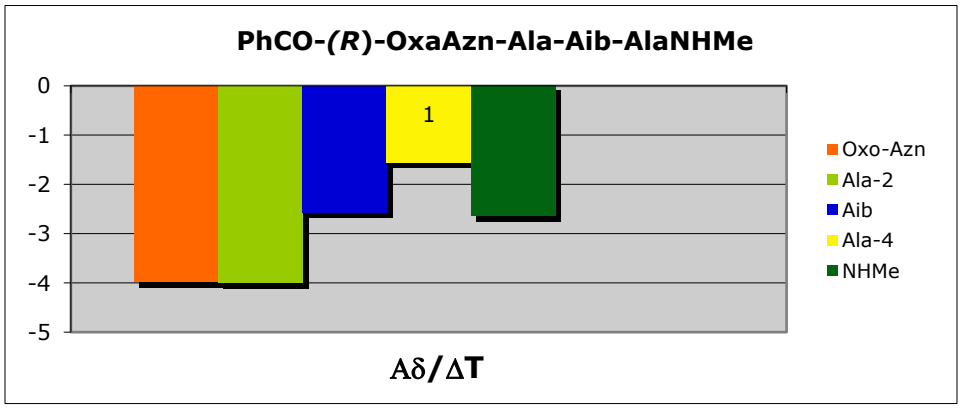

Figure 7. Temperature dependence of the NH proton chemical shifts.

This data suggest that NH of Aib, Ala-4, and NHMe fall within the typical ranges for

intramolecularly H- bonded protons. Conversely, an equilibrium between an intramolecularly H-bonded and a non-H-bonded state is suggested for the NH moieties of PhCONH and Ala-2 on the basis of temperature dependences of about 4 ppb K^{-1} (Figure 7).

From these findings we can postulate that a regular 3_{10}-helix construct, stabilized by three consecutive, $i + 3 \rightarrow i$ N-H···O=C intramolecular H-bonds (NH-3/PhCO, NH-4/COOxo_Azn-2, and NHMe/CONHAla2) was formed. On the other hand, differently to similar compounds reported in the literature[12], we did not detect any intramolecular H-bond between the heterocyclic CO group and the oxoazepane NH that could compete to the induction of helix conformation. Therefore it has to be stressed the ability of oxa-Azn to strongly stabilize 3_{10}-helix even if in very short peptides.

*Molecular Dynamics (MD) studies on model peptide **10**.* To evaluate the folding behavior of (R)-Oxo-Azn, we also performed Replica Exchange Molecular Dynamics (REMD) simulations starting from a fully extended conformation of peptide **10** (φ = ψ = ω = 180°), accordingly to the protocol reported in our previous studies.[8a,9c] The resulting trajectory, extracted from each replica in order to simulate a constant temperature of 308.5 K, was then analyzed in terms of H-bonds, secondary structure and cluster analyses (Tables 1-3, Figure 8).

Table 1. Results of DSSP analysis of the 100 ns REMD trajectory obtained at T = 308.53 K

#Residue	3_{10}-helix	α-helix	Turn
oxo-AZN1	0.3111	0.0364	0.1971
Ala2	0.3466	0.0364	0.2577
Aib3	0.3466	0.0364	0.3149
Ala4	0.1874	0.0364	0.2997

Table 2. Results of H-Bond analysis of the 50-100 ns REMD trajectory at T = 308.53 K

Acceptor	Donor	Occ%	AvgDist[a] (Å)	AvgAng[b] (deg.)

Ph C=O	Aib3 NH	37.0	3.20	163.1
Ala2 C=O	NHMe	27.0	3.13	160.5
oxo-Azn1 C=O	Ala4 NH	19.1	3.32	162.0
ARS1 C=O	NHMe	5.3	3.13	161.9
Ph C=O	Ala4 NH	3.9	3.42	162.9

[a]Donor-acceptor distance; cutoff = 4.0 Å. [b]Donor-H-acceptor angle; cutoff = 150 deg.

Table 3. Average dihedrals obtained from the analysis of the three most populated cluster trajectory

	#1	#2	#3	#4	#5
φ1	-28.6±34.6	15.6±43.1	22.1±41.0	-16.1±43.0	33.3±28.5
ψ1	-33.0±34.6	18.2±47.2	22.5±46.5	-20.3±43.4	35.1±31.6
φ2	-59.8±26.3	-87.3±48.1	-92.6±40.0	-63.6±40.5	34.8±43.6
ψ2	-22.3±19.1	110.7±80.5	132.4±68.8	3.7±46.1	31.7±17.0
φ3	-44.8±12.5	-22.2±37.8	39.6±18.6	22.0±37.6	46.4±9.0
ψ3	-43.6±29.2	-23.7±54.7	26.9±62.7	6.6±72.0	43.2±16.0
φ4	-85.2±26.7	-86.9±35.4	-74.6±60.0	-86.9±44.2	-77.8±54.8
ψ4	16.2±65.3	49.4±81.4	87.3±86.4	79.6±91.2	69.6±91.8

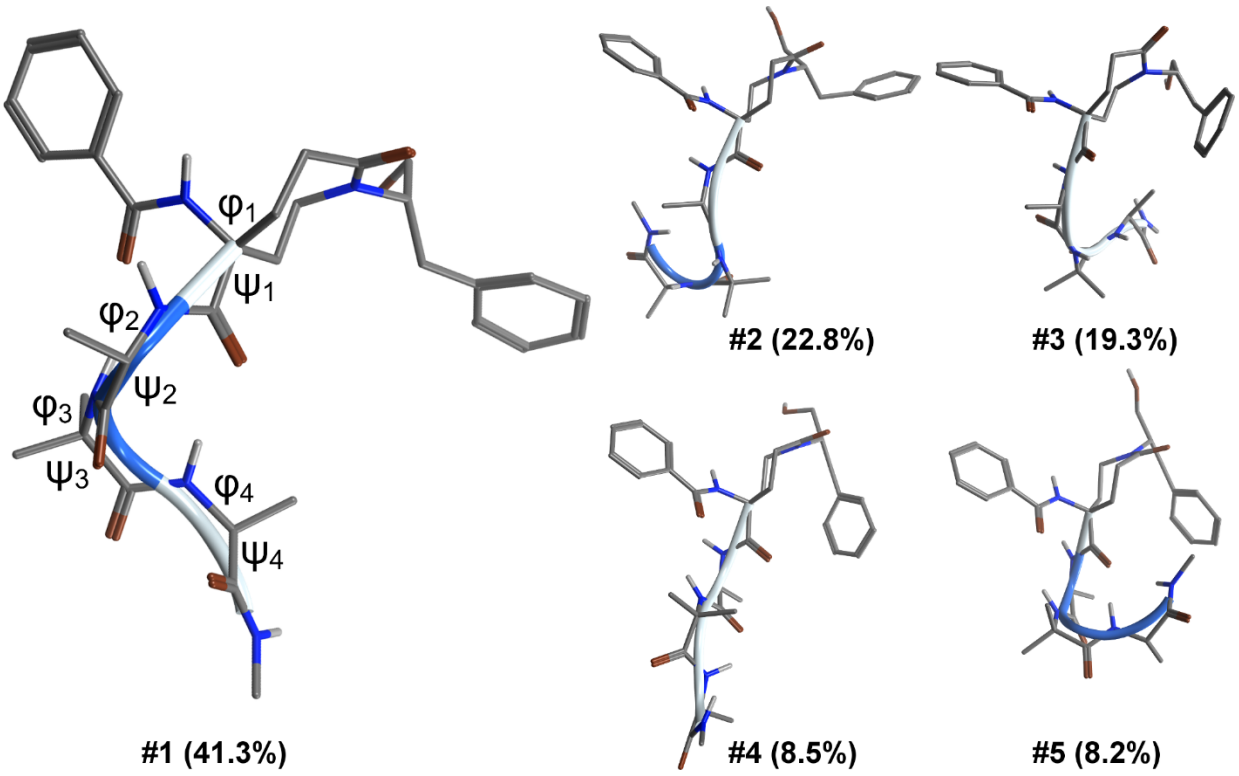

Figure 8. Representative structure and relative population (%) of the most populated clusters obtained by cluster analysis of the 50-100ns REMD trajectory obtained at T = 308.53 K

Results show that oxo-Azn has an helical propensity similar to that observed for the parent **Azn**[8a,9c] suggesting that neither the lactame C=O nor the substituted chain at the azepine N negatively affect the ability to stabilize helical conformations. Indeed, the DSSP analysis of the REMD 308.53 K (Table1) trajectory shows a relatively high helical content for residues 1-3, with turn content being prevalent only for the C-terminal residue Ala4. It can also be observed that the helical content is principally due to 3_{10} helix conformation, with only a marginal contribution of α-helix. This is also confirmed by H-bond analysis (Table 2), since relevant H-bonds are those of the i → i+3 type (Ph C=O···HN Aib3, oxo-Azn C=O···HN Ala4 and Ala2 C=O···HNMe), typical of 3_{10} helices, while i → i+4 H-bonds show occupancies of about 5%. Finally, geometrical clusterization (Figure 8) followed by the analysis of relevant φ and ψ dihedrals (Table 3) showed an helical conformation as the well-defined secondary structure most frequently sampled during the simulation (cluster #1, pop% = 41.3, Figure 8), even if structures classifiable as different folding intermediates (clusters #2-5) represent about the 60% of the

whole conformational population. By observing the average φ and ψ values of the most populated cluster #1, it can be observed that most dihedrals fall within the range typical of 3_{10} helix (even if an α-helix cannot be excluded, if deviations from the average values are considered).[13] Further details on the folding preferences of peptide **10** were also provided by the analysis of the 3D Ramachandran plot derived from the 100 ns REMD trajectory obtained at 308.53 K (Figure 9).

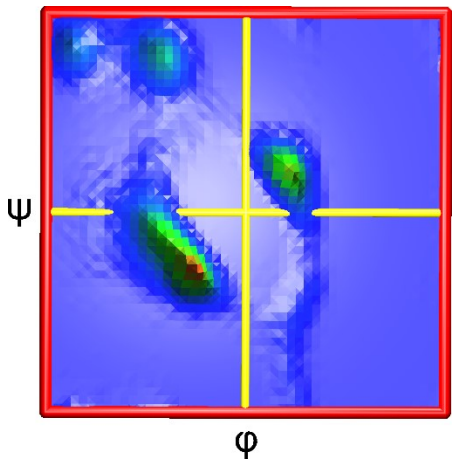

Figure 9. 3D Ramachandran plot obtained from the 100 ns REMD trajectory (308.53 K) of peptide 10. The z-axis represents the frequency of occurrence.

It can be observed that the most frequently sampled couple of φ and ψ dihedrals is that typical of the right-handed helix secondary structure, followed by a not negligible amount of left handed helix. Dihedral values belonging to the β regions are also sampled and, interestingly, the paths connecting the different regions of the 3D-Ramachandran plot can also be observed as ruffles on the graph surface, which indicate high energy conformations which are only occasionally sampled.

*Use of scaffold **5** for gold nanoparticles preparation.* Finally, we investigated the possibility of using scaffold **5** for the obtainment of covered gold nanoparticles.

First, we introduced a thiol tether through an ester linkage with the hydroxy function of scaffold **5**. Tritylsulfanyl-propionic acid was condensed with scaffold **5** using DCC and DMAP (CH_2Cl_2, 25 °C, h) affording compound **12** (80%, Scheme 3).

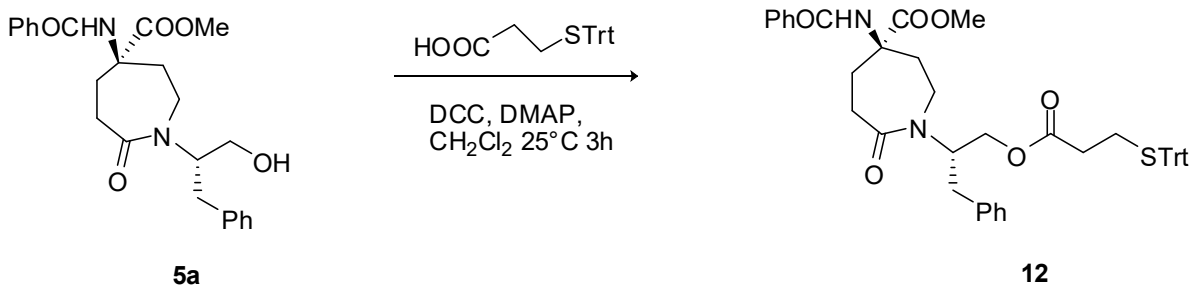

5a **12**

Scheme 3. Condensation between **5a** and 3-tritylsulfanyl propionic acid.

Gold nanoparticles (1-2 nm diameter) were prepared by chemical reduction (with $NaBH_4$) in a methanol/water mixture of the corresponding tetracloroidrate salts in the presence of the amino acid conjugate **12**.[6b]

The resulting dark-brown nanoparticle conjugated are well soluble in CH_2Cl_2 and $CHCl_3$. TEM analysis (Figure 10) revealed the formation of nanoparticles with metallic core of diameter ranging between 1.5-2.0 nm (Figure 11) .

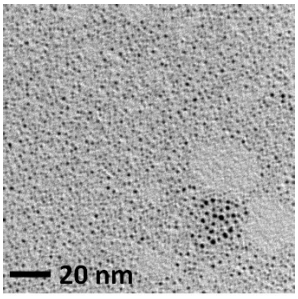

Figure **10**. TEM images of **12-AuNps** conjugate

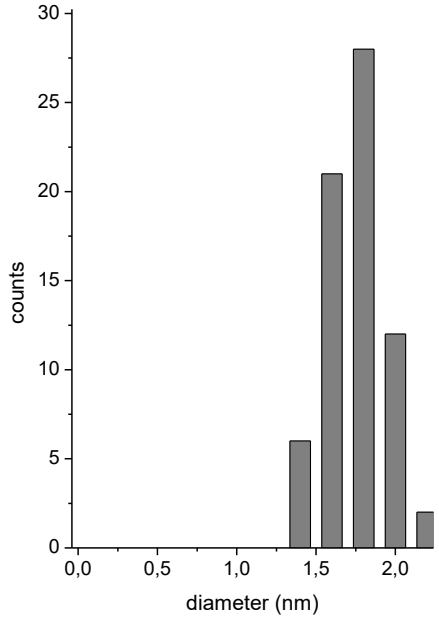

Figure **11**: Histograms showing the core size distribution of 1-AuNps conjugate.

Furthermore, dynamics light scattering (DLS) and UV-Vis absorption spectra (both recorded in CH_2Cl_2 solution) supported the formation of such nanoparticles (Figure 12 e 13). In particular DLS reveled 5 nm particle size distribution, which are in according with the ligand size while UV-Vis absorption spectra showed a moderate plasmatic band with a maximum at 530 nm, typical for 2 nm gold nanoparticle. Moreover, IR (KBr) analysis showed typical amide bond signals [*v*: 3297 (NH-amides), 1734 (CO esters), 1651 (CO amide I), 1546 (CO amide II) cm^{-1}] that confirmed the occurrence of metal-[1]conjugation and the preservation of the functional groups of **5a**.

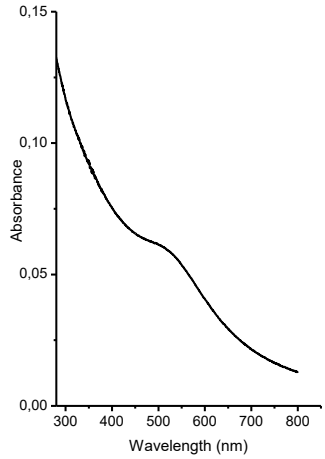

Figure **12**: UV-Vis spectra of **12-AuNps** conjugate recorded in CH_2Cl_2 solution the 380-800 nm region

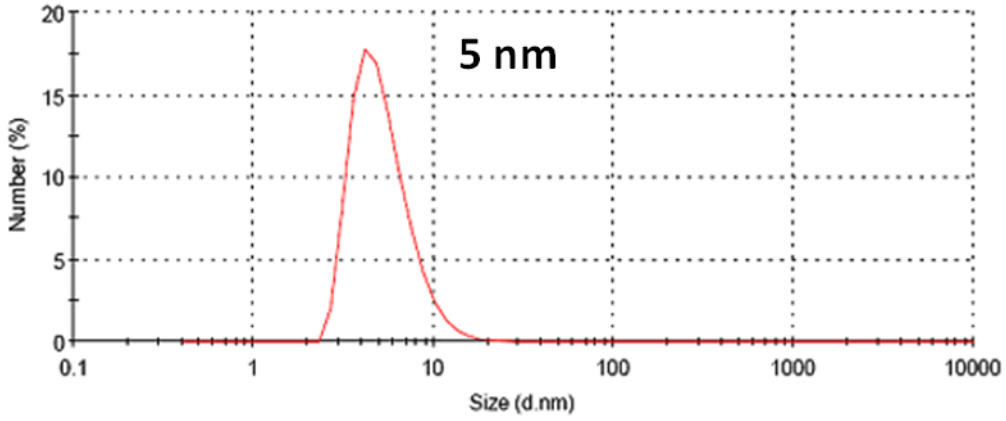

Figure **13**: Light scattering data obtained for **12-AuNps** in CH_2Cl_2 solution

In conclusion, the new glutamine analogue **oxo-Azn** functionalized on the nitrogen side chain with an hydroxyalkyl tether was efficiently synthesized in enantiopure form and in gram scale by an asymmetric one step procedure. Both theoretical and dynamic NMR studies revealed that R-**oxo-Azn** is a good 3_{10}-helix inducer when inserted in short peptide sequence. Finally, the presence of the tethering group allowed the preparation of functionalized gold nanoparticles.

EXPERIMENTAL SECTION

Theoretical calculations

The materials and solvents were purchased from common commercial sources and used without additional purification. ^{1}H NMR spectra were recorded at 200, 400 or 500 MHz and ^{13}C NMR spectra at 50, 70 or 125 MHz using TMS as internal standard. The following abbreviations were used to describe peak patterns where appropriate: singlet (s), doublet (d), triplet (t), multiplet (m), broad resonances (br). Coupling constants (J) are reported in hertz. Mass spectroscopy data of the products were collected on TERMOFININGAN LCQ ADVANTAGE source API ESI instrument. Infrared spectra were recorded on a FTIR spectrometer Perkin-Elmer 16 PC. $[\alpha]_D$ Values were measured with Perkin Elmer 343 plus polarimeter using $CHCl_3$ as the solvent, if not differently reported.

General Procedure for the Schmidt Reaction. *Method A)* Ketone **1**[9c] (11g, 40 mmol) was dissolved in dry CH_2Cl_2 (300 mL) under nitrogen atmosphere. After cooling at -10°C, $BF_3(OEt)_2$ (26.5 mL, 200 mmol) was dropped and the mixture was stand for 30 min after which azide **2a** or **2b** (1.3 equiv.), dissolved in CH_2Cl_2 (200 mL) was added. The stirring was continued (TLC: CH_2Cl_2/MeOH, 10:1) and the temperature was gradually increased to 25°C in 18h period. A solution of NaOH (2N, until pH 14) was added and the mixture was stirred for 30 min.. A white solid, corresponding to the isomer **6a** or **6b**, was formed and filtered. The organic layer was separated and the aqueous one was extracted with CH_2Cl_2 (3 x 50 mL). The organic layers were washed with a saturated solution of NH_4Cl (pH 4). After drying over Na_2SO_4 and solvent evaporation, the crude mixture was chromatographed on silica gel affording diastereoisomers **5** and **6**. *Method B)*. The reaction of azide **2a** (275 mg, 1.3 mmol) and ketone **1** (300 mg, 1.1 mmol) was performed according to point *a)* but avoiding the quenching with NaOH. After solvent evaporation, ^{1}H NMR analysis of the crude mixture showed the formation of a mixture of **3a**/**4a** in 67:33. The reaction mixture was taken up with Et_2O affording pure compound **4a** (60

mg, 13%). The mother liquors were chromatographed (CH_2Cl_2/MeOH, from 100:0 to 50:1) affording **5a** (210 mg, 45%) and **6a** (50mg 10%).

Methyl 4-Benzoylamino-1-[(*S*)-1-hydroxy-3-phenylpropan-2-yl]-7-oxoazepan-4-carboxylate (5a/6a): 67:33. Column chromatoghraphy codntion:CH_2Cl_2/MeOH, from 100:0 to 10:1

(*R*)-**5a**: 47%. Mp 234 °C (CH_2Cl_2/MeOH); $[\alpha]_D^{25}$ -24.7 (*c* 0.02, DMSO); IR (KBr) ν_{max} 3340, 1723, 1660 cm^{-1}; ^1H NMR (DMSO-d_6, 500 MHz) δ 8.55 (s, 1H, exch.), 7.84 (d, *J* 7.1, 2H), 7.57-7.18 (m, 8H), 4.77 (t, *J* 5.3, 1H, exch.), 4.74 (brs, 1H), 3.56 (s, 3H, OMe), 3.54-3.48 (m, 2H), 3.45-3.39 (m, 1H), 3.35-3.27 (m, 1H), 2.86 (dd, *J* 15.2, 6.3, 1H), 2.75 (dd, *J* 15.2, 9.5,1H), 2.65-2.55 (m, 1H), 2.30-2.18 (m, 2H), 2.14-2.05 (m, 1H), 1.85-1.68 (m, 2H); ^{13}C NMR (DMSO-d_6, 125 MHz) δ 28.2, 31.3, 34.1, 34.6, 38.2, 51.7, 55.8, 59.9, 60.9, 125.7, 127.5 (x2), 127.9 (x4), 128.4 (x2), 131.2, 133.8, 138.6, 166.6, 173.4, 173.9; MS (ESI+) 447.3 [M+23] $C_{24}H_{28}N_2O_5$ Calcd for: C, 67.91; H, 6.65; N, 6.60; Found: C, 67.78; H, 6.80; N, 6.49.

(*S*)-**6a**: 23%. Mp 230 °C dec. (CH_2Cl_2/*n*-hexane); $[\alpha]_D^{25}$ -47.7 (*c* 0.01, DMSO); ν_{max} 3435, 1737, 1627cm^{-1}; ^1H NMR (DMSO-d_6, 500 Mz) δ 8.51 (s, 1H, exch.), 7.82 (d, *J* 7.1, 2H), 7.58-7.15 (m, 8H), 4.75 (t, *J* 4.8, 1H, exch.), 4.54 (brs, 1H), 3.58 (s, 3H), 3.55-3.42 (m, 3H), 3.35-3.22 (m, 1H), 2.24-2.71 (m, 2H), 2.66 (dd, *J* 13.1, 13.6, 1H), 2.38-2.28 (m, 1H), 2.25-2.07 (m, 2H), 1.83 (dd, *J* 13.5, 12.8, 1H), 1.81-1.70 (brs, 1H); ^{13}C NMR (DMSO-d_6, 125 Mz) δ 28.2, 31.2, 34.1, 34.3, 39.1, 51.7, 57.8, 60.1, 60.9, 125.7, 127.5 (x2), 127.9 (x2), 127.9 (x2), 128.6 (x2), 131.2, 133.9, 138.8, 166.9, 173.6, 173.9; MS (ESI+) 447.2 [M+23] $C_{24}H_{28}N_2O_5$ Calcd for: C, 67.91; H, 6.65; N, 6.60; Found: C, 67.78; H, 6.80; N, 6.49.

Methyl 4-Benzoylamino-1-[(S)-2-hydroxy-1-phenylethyl]-7-oxoazepan-4-carboxylate (5b/6b): 50:50. Column chromatoghraphy condition :CH_2Cl_2/MeOH, from 100:0 to 50:1

(*R*)-5b: 35% Mp 260 °C (CH_2Cl_2/MeOH); $[\alpha]_D^{25}$ +13.23 ($2.04 \cdot 10^{-3}c$, MeOH); IR (KBr)ν_{max}3359, 1726, 1624 cm^{-1}; ^1H NMR (DMSO-d_6, 300 MHz) *δ*8.58 (s, 1H, exch), 7.84 (d, *J* 8.2, 2H), 7.58-7.25 (m, 8H), 5.63 (t, *J* 6.8, 1H),4.93 (brs, 1H, exch), 3.88 (t, *J* 4.7, 2H), 3.54 (s, 3H), 3.56-3.54; 3.30-3.20 (2 m, 2H), 2.74 (dd, *J* 2.5, 2.0, 1H), 2.55-2.25 (m, 2H), 2.10-1.85 (m, 2H), 1.50 (br, 1H); ^{13}C NMR (DMSO-d_6, 75 Mz) *δ*29.6, 32.3, 35.5, 39.3, 52.8, 58.0, 60.6, 61.0,

128.1, 128.6 (x2), 128.7 (x2), 129.0 (x2), 129.2 (x2), 132.3, 134.9, 139.5, 167.7, 174.5, 174.9; **MS** (ESI+) 411.2 [M+1], 433.3 [M+23] $C_{23}H_{26}N_2O_5$,Calcd for: C, 67.30; H, 6.38; N, 6.82; Found: C, 67.01; H, 6.55; N, 6.63.

(*S*)-6b: (trace amount of **7a** are present); IR (KBr)ν_{max}3412, 1738, 1627 cm^{-1}; ^1H NMR (DMSO-d_6, 300 MHz) δ8.49 (s, 1H, exch.), 7.85 (d, *J* 7.2, 2H, arom.), 7.56-7.20 (m, 8H, arom.), 5.66 (dd, *J* 13.8, 5.9, 1H, *CH*Ph), 4.93 (t, *J* 4.8, 1H, exch. OH), 4.00-3.75 (m, 2H, CH_2OH), 3.60 (s, 3H, OMe), 3.53 (dd, *J* 15.9, 10.1, 1H, CHN), 3.13 (dd, *J* 15.9, 6.1, 1H, CHN), 2.89 (t, *J* 13.5, 1H, CH_2CO), 2.60-2.40 (m, 1H, CH_2CH_2CO), 2.28 (dd, *J* 14.5, 8.3, 1H, CHCO), 2.25-2.10 (m, 1H, CH_2CH_2N), 2.10-1.85 (m, 2H, $CHCH_2CO$, CH_2CH_2N); ^{13}C NMR (DMSO-d_6, 75 MHz) δ29.1, 32.1, 35.8, 39.4, 52.9, 57.9, 60.5, 61.3, 127.9, 128.4 (x2), 128.7 (x2), 129.0 (x2), 129.2 (x2), 132.2, 135.0, 139.7, 167.9, 174.8, 175.5; MS (ESI+) 411.4 [M+1], 433.4 [M+23],$C_{23}H_{26}N_2O_5$. Calcd for: C, 67.30; H, 6.38; N, 6.82; Found: C, 66.97; H, 6.54; N, 6.58.

Methyl 7-benzoylamino-(*S*)-3-benzyl-3,5,6,7,8,9-hexahydro-oxazolo[3,2-*a*]azepinium-7-carboxylate · BF_4^- (3a/4a): 67:33.

(*R*)-**3a** (mixture with (*S*)-**4a)**: ^1H NMR ($CDCl_3$, 500 MHz) main signals: δ 7.92 (d, *J* 7.1, 2H), 4.91 (m, 1H), 4.70 (m, 1H), 4.68 (m, 1H), 4.10-4.00 (m, 1H), 3.69 (s, 3H, OMe), 2.00-1.70 (m, 2H); ^{13}C NMR ($CDCl_3$, 125 MHz) δ 23.1, 27.7, 29.7, 32.1, 36.7, 42.5, 53.1, 60.2, 65.6, 76.3, 127.6 (x2), 127.9, 128.6 (x2), 129.2 (x2), 129.4 (x2), 132.2, 132.8, 133.5, 167.9, 173.1, 179.0.

(*S*)-**4a**: ν_{max} 3400, 1738, 1661 cm^{-1};^1H NMR ($CDCl_3$, 500 MHz) δ 7.88 (d, *J* 7.2, 2H), 7.50-7.46 (m, 1H), 7.42-7-37 (m, 5H), 7.36-7.33(m, 1H), 7.22 (d, *J* 6.9, 2H), 5.03 (dd, *J* 9.8, 9.3, 1H), 4.97-4.90 (m, 1H), 4.68 (dd, *J* 9.3, 5.9, 1H), 3.98 (dd, *J* 15.1, 8.5, 1H), 3.81 (dd, *J* 15.1, 9.3, 1H), 3.74 (s, 3H), 3.25 (dd, *J*14.4, 5.0, 1H), 3.09 (dd, *J* 17.7, 10.3, 1H), 3.04 (dd, *J* 14.4, 7.5, 1H), 2.86 (dd, *J* 17.7, 8.8, 1H), 2.82 (dd, *J* 16.7, 9.2, 1H), 2.67 (ddd, *J* 16.3, 9.0, 1.6, 1H), 2.30-2.59 (dd, *J* 15.6, 8.3 1H), 2.54 (ddd, *J* 16.3, 13.5, 1.8, 1H); ^{13}C NMR ($CDCl_3$, 125 MHz) δ 21.9, 26.4, 31.4, 36.3, 41.8, 52.3, 59.2, 64.6, 75.5, 126.8(x2), 127.5, 127.9 (x2), 128.5 (x2), 128.8 (x2), 131.4, 132.1, 132.2, 166.9, 172.2, 178.6; MS (ESI+) 407.3 $[M]^+$ $C_{24}H_{27}N_2O_4$.

(*R*)-4-Benzoylamino-1-[(*S*)-1-hydroxy-3-phenylpropan-2-yl]-7-oxoazepane-4-carboxylic acid (7). Ester **5a** (300 mg, 0.7 mmol) was dissolved in CH_2Cl_2/MeOH (9:1, 10.5 mL). A 2N methanolic solution of NaOH (1.13 mL) was added and the mixture was stirred at 25 °C for 15 h (TLC: CH_2Cl_2/MeOH, 10:1). After solvent evaporation, the mixture was taken up with H_2O and acidified 12 N with HCl until pH 1. A solid was separated and filtered corresponding to acid **7** (220 mg). The aqueous solution was extracted with CH_2Cl_2 (3 x 3 mL). The organic layers were then dried over Na_2SO_4 and the solvent was removed under vacuum. After crystallization, a further crop of pure compound **7** was obtained (50 mg). Acid **7** was obtained in 95% overall yield.

Mp: 180 °C (Et_2O); $[\alpha_D]^{25}$ +18.3 (*c* 0.1, MeOH); IR (KBr) ν_{max} 3353, 2923, 1720 cm^{-1}; ^1H NMR (DMSO-d_6, 300 MHz) δ 12.28 (brs, 1H), δ 8.40 (s, 1H), δ 7.84 (d, *J* 7, 2H), δ 7.37 (m, 8H), δ 4.70 (m, 1H), δ 4.30 (brs, 1H), δ 3.46 (m, 4H), δ 2.80 (m, 2H), δ 2.52 (m, 1H), δ 2.20 (m, 3H), δ 1.89 (m, 2H); ^{13}C NMR (DMSO-d_6, 75 MHz) δ 23.3, 27.8, 29.3, 31.6, 32.5, 35.2, 35.8, 36.7, 42.1, 57.2, 60.8, 61.0, 61.9, 65.4, 126.8, 128.5, 128.9, 129.5, 132.1, 135.2, 139.7, 175.1, 175.4; MS (ESI-) 409.6 [M-1]. $C_{23}H_{26}N_2O_5$ Calcd for : C, 67.30; H, 6.38; N, 6.82; Found: C, 67.13; H, 6.53; N, 7.01.

Synthesis of dipeptide 8. The (L)alanine benzyl ester *p*-toluenesulfonate (200 mg, 1.11 mmol) was suspended in CH_2Cl_2 (5 mL) and then treated with triethylamine (155 μL, 1.11 mmol). The mixture was washed with H_2O. The organic layers were dried over Na_2SO_4 and the solvent was evaporated under vacuum. Acid **7** (130 mg, 0.320 mmol) was dissolved in a CH_2Cl_2 (3.2 mL)/DMF (0.1 mL) mixture. After cooling to 0°C, HOAt (44 mg, 0.320 mmol), EDC (61 mg, 0.320 mmol), alanine benzyl ester (170 mg, 0.950 mmol) and DIPEA (2 equiv., 0.112 mL, until pH 8) were added to the mixture. The reaction was left under stirring overnight at 25 °C (TLC: CH_2Cl_2/MeOH, 10:1). The mixture was washed with aqueous 3N HCl (2 x 5 mL), H_2O (5 mL) and finally with $NaHCO_3$ (2 x 5 mL). The organic layer was dried over Na_2SO_4 and the solvent was evaporated under vacuum. The crude mixture was crystalized affording pure compound **13** (185 mg, 80%). Mp: 120 °C (CH_2Cl_2/Et_2O); $[\alpha_D]^{25}$ -27.5 (*c* 0.1, MeOH); IR (KBr) ν_{max} 3400, 1740 cm^{-1}; ^1H NMR ($CDCl_3$, 300 MHz) δ 7.77 (d, *J* 6.90, 2H), 7.31 (m, 14 H), 7.01 (s, 1H), 5.11 (q, *J* 11.91 , 2H), 4.70 (brs, 1H), 4.53 (t, *J* 14.07, 1H), 3.64 (m, 2H), 3.36 (m, 2H), 2.69 (m, 4H), 2.15 (m, 4H), 1.33 (m, 3H), 1.27 (s, 1H); ^{13}C NMR ($CDCl_3$, 75 MHz) δ 176.4, 173.1, 172.9,

168.4, 138.2, 135.7, 134.4, 132.3, 129.8, 129.3, 129.1, 129.0, 128.9, 128.7, 128.6, 128.5, 128.4, 127.7, 127.4, 127.2, 127.0, 67.4, 63.1, 61.6, 59.5, 48.8, 40.9, 36.1, 35.2, 32.3, 29.3, 18.3, 10.0; MS (ESI-) 570.9 [M-1]. $C_{33}H_{37}N_3O_6$ Calcd for: C, 69.33; H, 6.52; N, 7.35; Found: C, 69.57; H, 6.23; N, 7.04.

Debenzylation of ester 8. Ester **8** (100 mg, 0.175 mmol) was dissolved in MeOH (5 mL). Pd/C (185 mg, 0.175 mmol) was added and the mixture was hydrogenated at 25 °C overnight (TLC: CH_2Cl_2/MeOH, 10:1). The catalyst was filtered on a celite pad and acid **9** (75 mg, 90%) was obtained after crystallization. Mp: 140°C (CH_2Cl_2/Et_2O); $[\alpha_D]^{25}$ -20.83 (*c* 0.2, MeOH); IR (KBr) ν_{max} 3400, 2928, 1730, 1629 cm^{-1}; ^1H NMR (CD_3OD, 300 MHz) δ 7.83 (m, 2H), 7.50 (m, 3H), 7.25 (m, 6H), 4.32 (q, *J* 7.11, 1H), 3.69 (m, 2H), 3.55 (brs, 2H), 3.33 (m, 2H), 2.85 (m, 2H), 2.51 (m, 3H), 2.14 (m, 3H), 1.33 (m, 4H); ^{13}C NMR **(**CD_3OD, 75 MHz) δ 176.8, 175.8, 174.1, 169.5, 138.5, 134.8, 131.8, 129.1, 128.8, 128.5, 127.7, 127.6, 127.5, 126.5, 61.6, 58.6, 49.2, 48.6, 48.1, 47.7, 39.8, 35.6, 34.8, 31.8, 28.3, 17.2; MS (ESI+) 504.3 [M+23]. $C_{26}H_{31}N_3O_6$ Calcd. for: C, 64.85; H, 6.49; N, 8.73; Found: C, 64.56; H, 6.78; N, 8.46;

Synthesis of tetrapeptide 10. Acid **9** (60 mg, 0.125 mmol) was suspended in a mixture CH_2Cl_2 (1.25 mL)/DMF (0.1 mL). After cooling to 0°C, HOAt (17 mg, 0.125 mmol), EDC (24 mg, 0.125 mmol), dipeptide H_2N-Aib-(*L*)-AlaNHMe (60 mg, 0.312 mmol) and DIPEA (2 equiv., 0.044 mL, until pH 8) were added to the mixture. The reaction was stirred at 25°C overnight (TLC: CH_2Cl_2/MeOH, 10:1). The mixture was washed with aqueous 3N HCl (2 x 5 mL), H_2O (1x 5 mL) and finally with $NaHCO_3$ (2 x 5 mL). The organic layer was dried over Na_2SO_4 and the solvent was evaporated under vacuum. The crude mixture was crystalized from CH_2Cl_2/Et_2O affording crude peptide **10** (40 mg, 50%). A further purification was performed by HPLC (phase A: 95% H_2O, 5% CH_3CN, 1 mL TFA; phase B: 95% CH_3CN, 5% H_2O, 1 mL TFA; elution gradient: 95% A for 5 min, then 95-30% A in 20 min) to give peptide **10** (20 mg, 25%). During the purification we observed the formation of a by-product, corresponding to the bicyclic derivative **11**. Pure peptide **10** (30 mg, 38%) can be obtained from the crude by performing a second crystallization from CH_2Cl_2/Et_2O.

10: Mp: 120°C (CH_2Cl_2/Et_2O); $[\alpha_D]^{25}$ +6.23 (*c* 0.2, MeOH); IR (KBr) ν_{max} 3400, 1740 cm^{-1}; ^1H NMR **(**CD_3CN, 300 MHz) δ 8.92 (s, 1H), δ 7.93 (d, *J* 7.2, 2H), δ 7.69 (d, *J* 10.9, 1H), δ 7.56 (m,

3H), δ 7.23 (m, 5H), δ 4.68 (brs, 1H), δ 4.06 (m, 1H), δ 3.90 (m, 1H), δ 3.49 (m, 8H), δ 3.03 (m, 1H), δ 2.71 (m, 1H), δ 2.66 (d, *J* 4.6, 2H), δ 1.97 (m, 7H), δ 1.69 (m, 6H), δ 0.85 (m, 6H); ^{13}C NMR **(**CD_3CN, 75 MHz) δ 212.96, 174.83, 160.38, 149.35, 132.43, 129.37, 128.80, 128.65, 128.21, 127.74, 126.51, 108.42, 66.72, 62.44, 54.51, 52.76, 50.07, 44.92, 40.73, 38.31, 34.81, 34.69, 31.96, 30.43, 29.74, 26.71, 25.67, 23.45, 17.29, 16.22, 13.36, 13.28, 10.52; MS (ESI+) 651.3 [M+1]. $C_{34}H_{46}N_6O_7$ Calcd. for: C, 62.75; H, 7.12; N, 12.91; Found: C, 62,56; H, 7.34; N, 13.17.

Synthesis of compound 12. Alcohol **5a** (0.26 mmol) was dissolved in CH_2Cl_2 (3 mL) and 3-tritylsulfanyl-propionic acid (100 mg, 0.286 mmol) was added. After cooling to 0°C, DMAP (3 mg, 0.026 mmol) was added and DCC (36 mg, 0.286 mmol) dissolved in CH_2Cl_2 (1 mL) was dropped to the solution. The reaction was stirred for 3h at 25 °C (TLC: CH_2Cl_2/AcOEt, 1:1). The mixture was washed with $NaHCO_3$ (1 x 5 mL) and H_2O (1 x 5 mL). The organic layers were dried over Na_2SO_4 and the solvent was evaporated under vacuum. Pure compound **12** was obtained after crystallization.

(*R*)-Methyl 4-benzoylamino-7-oxo-1-[(S)-1-phenyl-3-((3-(tritylthio)propanoyl)oxy)propan-2-yl)azepane-4-carboxylate (12): 80%. Mp: 80°C (AcOEt/Et_2O); $[\alpha_D]^{25}$ -8.75 (*c* 0.0016, MeOH); IR (KBr) ν_{max} 3326, 1738 cm^{-1}; ^{1}H NMR ($CDCl_3$, 200 MHz) δ 10.09 (brs, 1H), 7.74 (m, 2H), 7.35 (m, 20H), 6.09 (s, 1H), 4.29 (m, 1H), 4.09 (m, 2H), 3.69 (m, 3H), 3.39 (m, 2H), 2.86 (m, 2H), 2.59 (m, 2H), 1.95 (m, 4H), 1.34 (m, 6H); ^{13}C NMR ($CDCl_3$, 75 MHz) δ 24.5, 24.7, 25.3, 25.4, 26.1, 27.1, 29.5, 29.8, 30.7, 31.9, 33.2, 33.8, 34.1, 35.0, 35.3, 50.5, 52.8, 60.6, 60.8, 64.3, 67.2, 114.2, 126.9 (x2), 127.2, 127.4, 127.9, 128.1, 128.4, 128.7, 128.8, 129.1, 129.2, 129.5, 129.7, 129.8, 132.1, 134.0, 137.6, 144.7, 147.1, 157.8, 167.4, 171.7, 173.2, 174.9; MS (ESI+) 777.5 [M+23]. $C_{46}H_{46}N_2O_6S$ Calcd for: C, 73.18; H, 6.14; N, 3.71; Found: C, 72.91; H, 6.35; N, 3.65.

Prepration of covered gold nanoparticles. H-S-[**12**] [obtained by Trt deporotection (50% TFA/CH_2Cl_2, 1% TIS) of the corresponding S-protected-[**12**] (150 mg, 0.19 mmol) and $HAuCl_4$ (38 mg, 0.1 mmol) were combined in 10 ml of a 1:1 methanol/water solvent mixture. The resulting solution was allowed to stand for 1 h, under stirring. Then 10 equivalents of $NaBH_4$ (1.65 ml of a 600 mM solution in water) were added and the solution was stirred at room temperature for additional 3 hrs. The product was precipitated by adding 3 vol. of CH_3CN,

pelleted for 8 min at top speed in a centrifuge, resuspended in 80% Et_2O/EtOH, pelleted again, and dried overnight at room temperature.

ASSOCIATED CONTENT

Supporting Information. A CIF file giving X-ray data for **4a**, NMR data for compounds **4a**, **10**, **11**. ^{1}H, ^{13}C NMR spectra for all new compounds. This material is available free of charge via the Internet at http://pubs.acs.org.

Corresponding Author

*e-mail: sara.pellegrino@unimi.it

Present Addresses

† Università degli Studi di Milano-DISFARM-Sez. Chimica Generale e Organica "A.Marchesini"-via Venzian 21-20133-Milano-Italy

§ Indirizzo Moretto

‡Raffaella: CNR- Istituto di Scienze e Tecnologie Molecolari-Via Golgi 19 - 20133 Milano-Italy.

Author Contributions

The manuscript was written through contributions of all authors. All authors have given approval to the final version of the manuscript.

ACKNOWLEDGMENT

Funding for this work was provided by MIUR (PRIN 2010-2011 - prot. 2010NRREPL).

REFERENCES

(1) a) Alex, S.; Tiwari, A. *J. Nanosci. Nanotec.*, **2015**, *15*, 1869-1894 b) Yongsheng M., Pengxia L., Zhou Y., Dong W., Wanli H., Hui C., Huai Y. *RSC Adv*., **2015**, *5*, 140-145; c). Figuero, E. R; Lina, A. Y.; Yana1, J.; Luoa, L.; Fosterb, A. E.; Drezek R. A. *Biomaterials*, **2014**, *35*, 1725–1734 d) Sapsford, K. E.; Algar, W. R.; Berti, L.; Boeneman Gemmill, K.; Casey, B. J.; Oh, E.; Stewart, M. H.; Medintz I. L. *Chem. Rev.* **2013**, *113*, 1904−2074 e) Jadhav, S. A. *J.Mater.Chem.,* **2012***, 22,* 5894*;* f) Prats-Alfonso, E.; Albericio, F. *J. Mater. Sci.,* **2011***, 46,* 7643–7648*;* g) Giljohann, D. A.; Seferos, D. S.; Daniel, W. L.; Massich; Patel, P. C.; Mirkin, C. A. *Angew. Chem., Int. Ed.*, **2010**, *49*, 3280–3294

(2) a) Osante, I.; Polo, E.; Revilla-Lo´pez, G.; de la Fuente, J, M.; Alema´n, C.; Cativiela, C.; Dı´az, D. *J Nanopart Res,* **2014**, *16*, 2224; b) Srisombat, L.; Jamison, A.C.; Lee, T.R. *Colloid Surf A*, **2011**, *39*0, 1–19

(3) Panda, J. J.; Chauhan, V S. *Polym. Chem.*, **2014**, *5*, 4418; b) Parween, S.; Misra, A.; Ramakumar, S.; Chauhan, V. S *J. Mater. Chem. B*, **2014**, *2*, 3096; c) Montenegro, A.; Ghadiri, V; Granja, J. R. *Acc. Chem. Res.* **2013**, *46*, 2955-2965 d) Hourani, R.; Zhang, C.; van der Weegen, R.; Changyi, L. R.; Keten, L. S.; Helms, B. A.; Xud, T. *J.Am.Chem.Soc.* **2011**, *133*, 15296– 15299; e) Lalatsa, A; Schätzlein, A. G.; Mazza, M.;. Hang Le, T. B.; Uchegbue, I. F. *J. Control. Rel.* **2012**, *161*, 523—553.

(4) a) Leea, E.-J.; Bea, C. L.; Vinsona, A. R., Richesa, A. G.; Fehra, F.; Gardinera, J.; Gengenbacha, T. R.; Winklera, D. A.; Haylock, D. *Biomaterials*, **2015**, *37*, 82–93; b) de Bruyn Ouboter, D.; Schuster, T. B.; Sigg, S. J.; Meier, W. P. *Colloids and Surfaces B: Biointerfaces* **2013**, *112*, 542-547

(5) Aili, D.; Gryko, P.; Sepulveda, B.; Dick, J. A. G.; Kirby, N.; Heenan, R.; Baltzer, L.; Liedberg, B.; O Mary, P. R.; Stevens, M. M. *Nano Lett.* **2011**, *11*, 5564–5573

(6) a) Parween, S.; Ali, A.; Chauhan, V. S *ACS Appl. Mater. Interfaces* **2013**, *5*, 6484-6493; b) Rio-Echevarria, I. M.; Tavano, R.; Causin, V.; Papini, E.; Mancin, F.; Moretto, A. *J. Am. Chem. Soc.* **2011**, *133*, 8-11; c) Aili, D.; Stevens, M. M. *Chem. Soc. Rev.*, **2010**, *39*, 3358–3370)

(7) Avan, I.; Hall, C. D.; Katritzky, A. R. *Chem.Soc.Rev.*, **2014**, *43* ,3575.

(8) a) Maffucci , I.; Pellegrino, S.; Clayden, J.; Contini, A. *J. Phys. Chem. B* **2015**, *119*, 1350-1361 b) Demizu, Y.; Doi, M.; Kurihara, M.; Okuda, H.; Nagano, M.; Suemune, H.; Tanaka, M. *Org. Biomol. Chem*. **2011**, *9*, 3303 – 3312 ; c) Gatto, E.; Porchetta, A.; Stella, L.; Guryanov, I.; Formaggio, F.; Toniolo, C.; Kaptein, B.; Broxterman, Q. B.; Venanzi, M. *Chem. Biodiversity* **2008**, *5*, 1263 – 1278 d) Tanaka, M. *Chem. Pharm. Bull*. **2007**, *55*, 349-358; e) Toniolo, C.; Crisma, M.; Formaggio, F.; Peggion, C.; Broxterman, Q. B.; Kaptein, B. *Biopolymers* **2004**, *76*, 162–176.

(9) a) Pellegrino, S.; Contini, A.; Gelmi, M.L.; Lo Presti, L.; Soave, R.; Erba, E. *J. Org. Chem*. **2014**, *79*, 3094-3102; b) Bonetti, A.; Clerici, F.; Foschi, F.; Nava, D.; Pellegrino, S.; Penso, M.; Soave, R.; Gelmi, M.L;. *Eur. J. .Org. Chem.*, **2014**, 3203-3209 c) Pellegrino, S.; Contini, A.; Clerici, F.; Gori, A.; Nava, D.; Gelmi, M. L. *Chem. Eur. J.* **2012**, *18*, 8705-8715; d) Penso, M.; Foschi, F.; Pellegrino, S.; Testa, A.; Gelmi, M.L. *J. .Org. Chem.*, **2012**, *77*, 3454-3461; e) Gassa, F.; Contini, A.; Fontana, G.; Pellegrino, S.; Gelmi, M.L. J. Org. Chem. **2010**, *75*, 7099-7106; f) S. Pellegrino, F. Clerici, M. L. Gelmi *Tetrahedron* **2008**, *64,* 5657-5665; g) Cabrele, C.; Clerici, F.; Gandolfi, R.; Gelmi, M.L.; Molinari, F.; Pellegrino, S. *Tetrahedron*, **2006**, *62*, 3502-3508.

(10) a) Ribelin, T.; Katz, C. E Withrow, D.; Smith, S.; Manukyan, A.; Day, V. W.; Neuenswander,B.; Poutsma, J. L.; Aubé, J. *Angew Chem, Int Ed* **2008**; *47*, 6233–6235; b) Katz, C. E.; Ribelin, T.; Withrow, D.; Basseri, Y.; Manukyan, A. K.; Bermudez, A.; Nuera, C. G.; Day, V. W.; Powell, D. R.; Poutsma, J. L.; Aubé, J. *J. Org. Chem.* **2008**, 73, 3318-3327; Katz, C. E; Aubé, J. *J. Am.. Chem. Soc.* **2003**, *125*, 13948-13949; Sahasrabudhe, K.; Gracias, V.; Furness, K.; Smith, B. T.; Katz, C. E.; Reddy, D. S.; Aubé, J. *J. Am. Chem. Soc.,* **2003**, *125*, 7914-7922 Gracias, V.; Frank, K.E., Milligan, G. L.; Aubé, J. *Tetrahedron*, **1997**, *53*, 16241-16252; Gracias, V.; Milligan, G. L.; Aubé, J. *J. Am. Chem. Soc.*, **1995**, *117*, 8047-8048

(11) Aib

(12) a) Nuñez-Villanueva, D.; Infantes, L.; García-Lopez, M. T.; Gonzalez-Muñiz, R.; Martín-Martínez, M. *J. Org. Chem.* **2012**, *77*, 9833-9839; b) Nuñez-Villanueva, D.; Infantes, L.; García-Lopez, M. T.; Gonzalez-Muñiz, R. *J. Org. Chem.* **2011**, *76*, 6592–6603

(13) An exception involved the terminal Ala4, that show a widened φ (averagely about -85 deg.) and a positive average ψ, although characterized by a high standard deviation which might mean a difficulty in the clusterization process, possibly due to an higher conformational variability of the C-terminal region respect to the remaining peptide.

For Table of Contents Only